Heliyon 9 (2023) e15503

Contents lists available at ScienceDirect

Heliyon

journal homepage: www.cell.com/heliyon

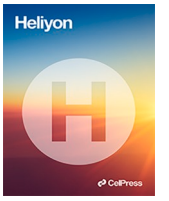

Research article

Preparation, characterization and antioxidant activity of cobalt polysaccharides from Qingzhuan Dark Tea

Hongfu Zhou [a,b,1], Yong Chen [a,b,1], Ziyao Wang [a,b], Chen Xie [a,b], Dan Ye [a,b], Anran Guo [a,b], Wenjing Xie [a,b], Jun Xing [a,b], Min Zheng [a,b,*]

[a] Xianning Medical College, Hubei University of Science and Technology, Xianning, Hubei, 437100, China
[b] Hubei Industrial Technology Research Institute of Intelligent Health, Xianning, Hubei, 437100, China

ARTICLE INFO

Keywords:
Qingzhuan Dark Tea
Polysaccharide
Cobalt complex
Antioxidant activity

ABSTRACT

The paradoxical effects of cobalt in biological processes have caused controversy regarding the application of cobalt-based biomaterials. Cobalt has recently been shown to be a trace element that promotes bone growth. Qingzhuan Dark Tea polysaccharides (TPS) has been shown to be a biomaterial with antioxidant and immunomodulatory effects. In order to develop a novel immunomodulatory biomaterial, we synthesized polysaccharide cobalt complex (TPS-Co) to prevent the paradoxical effects of cobalt while maintaining its beneficial effects, and evaluated its morphology, structure, and antioxidant activity. Fourier-transform infrared spectroscopy, X-ray diffraction and X-ray photoelectron spectroscopy demonstrated that cobalt complexed successfully with TPS. Scanning electron microscopy and atomic mechanical microscopy demonstrated that TPS-Co has a more homogeneous and concentrated morphological distribution compared to TPS. Thermal performance analysis demonstrated that TPS-Co has higher thermal stability. Atomic absorption spectroscopy showed a cobalt content of 3.8%. Ultraviolet spectroscopy indicated that TPS-Co does not contain nucleic acids and proteins. Antioxidant activity assays showed that TPS-Co has better antioxidant activity than TPS in the concentration range of 0.4–2 mg/mL. Proliferation assay of MC3T3-E1 cells demonstrated that TPS-Co has the best cell proliferation effect at a cobalt concentration of 2 ppm. Therefore, TPS-Co may have potential applications in bone regeneration.

1. Introduction

Cobalt, a component of vitamin B_{12}, has been proved in numerous studies to stimulate the hematopoietic system of the human bone marrow, promote the synthesis of hemoglobin and increase the number of red blood cells. However, due to its toxic effects, it cannot be widely used in the medical field. A recent study found that no systemic toxicity was observed at cobalt concentrations of 0.1–5 ppm in the body. 1 ppm of cobalt produced the best bone regeneration results [1]. Finding a way to maintain the beneficial effects of cobalt while preventing its toxic effects would be a valuable and rewarding strategy.

Qingzhuan Dark Tea is an important type of dark tea in China, mainly produced in Hubei, China. Recently, a variety of health benefits, including anti-obesity, antihyperlipidemic, antidiabetic, and antioxidant activities, have been demonstrated in dark tea and

* Corresponding author.
E-mail address: zhengminsci@163.com (M. Zheng).
[1] These authors have contributed equally to this work.

https://doi.org/10.1016/j.heliyon.2023.e15503
Received 16 August 2022; Received in revised form 6 April 2023; Accepted 11 April 2023
Available online 17 April 2023

its bioactive components [2]. Dark tea is gaining ever-growing popularity. One of the main components of its bioactivity is tea polysaccharide [3].

Natural plant polysaccharides can scavenge oxygen free radicals and reduce the damage to the human body. Because it is non-toxic or low-toxic, it has become a hot topic of research. Purple Sweet potato polysaccharide has a protective effect on liver injury induced by tris (2, 3-dibromopropyl) isocyanate [4]. However, the application of polysaccharides has some problems such as low oral bioavailability and low injection absorption. Because of their negative charge and anion exchange capacity, polysaccharides can be used as metal-binding platforms with specific physico-chemical properties and a variety of biological activities, such as astragalus polysaccharides and inorganic strontium. After compound treatment, polysaccharides form novel compounds with anti-inflammatory and bone formation therapy properties, allowing polysaccharides and strontium to synergistically promote bone regeneration [5]. When adding Cu_2O into algae polysaccharide, the complex showed higher conductivity and antibacterial activity than natural polysaccharide [6].

Tea is one of the top three beverages in the world. It is popular in all countries of the world and has a history of thousands of years. Compared with other natural plants, people are more receptive to tea, the active substances in tea are more easily absorbed and tolerated by the human body, and people have more confidence in the safety of tea. The advantage of using tea polysaccharides as a complexing platform for metal ions is that there are fewer adverse effects.

Therefore, we combined the polysaccharides of Qingzhuan Dark Tea with cobalt to form cobalt polysaccharides (TPS-Co for short). The aim of this study was to characterize the structure of TPS-Co and to investigate its antioxidant activity. The structural characterization and physical properties of TPS-Co were analyzed by molecular weight analysis, atomic absorption spectroscopy (AAS), thermogravimetric analysis (TGA), Fourier-transform infrared spectroscopy (FT-IR), ultraviolet spectroscopy (UV), scanning electron microscopy (SEM), X-ray diffraction (XRD), X-ray photoelectron spectroscopy (XPS), and atomic mechanical microscopy (AFM). The antioxidant activities of TPS and TPS-Co were compared by a series of in vitro experiments. Based on the cell proliferation assay of pre-osteoblast MC3T3-E1, we hypothesized that TPS-Co might have a better ability to promote bone regeneration less toxicity.

2. Materials and methods

2.1. Experimental materials

The Qingzhuan Dark Tea was obtained from Chibi city, Hubei Province, China. $CoCl_2$ (AR), 2,2-diphenyl-1-picrylhydrazyl, hydroxyl (DPPH), and 2,2'-azobis-3-ethylbenzothiazoline-6-sulfonic acid (ABTS) were procured from Macklin (China). MC3T3-E1 cells purchased from Procell Life Science & Technology Co., LTD. (China). Deionized water was used in all experiments unless otherwise stated.

2.2. Preparation of TPS

The tea powder was extracted using water for 4 h after degreasing and removing the small molecules. The supernatant was freeze-dried to obtain crude polysaccharides. First, 50 g of polyamide was soaked in 95% ethanol, 5% NaOH, and 10% hydrochloric acid for 4–5 h each in turn. Then, the polyamide resin was loaded into the column. The polyamide column was balanced after natural settlement, and TPS was dissolved in water. Further, the TPS was subjected to elution, decolorisation, and depigmentation to obtain the eluent. The refined polysaccharides were freeze-dried after 48 h of dialysis [7].

2.3. Preparation of the TPS-Co

Weigh 0.1 g of TPS and place it in a 50 mL cone flask with a constant volume of deionized water. Then it was placed in a 30 °C water

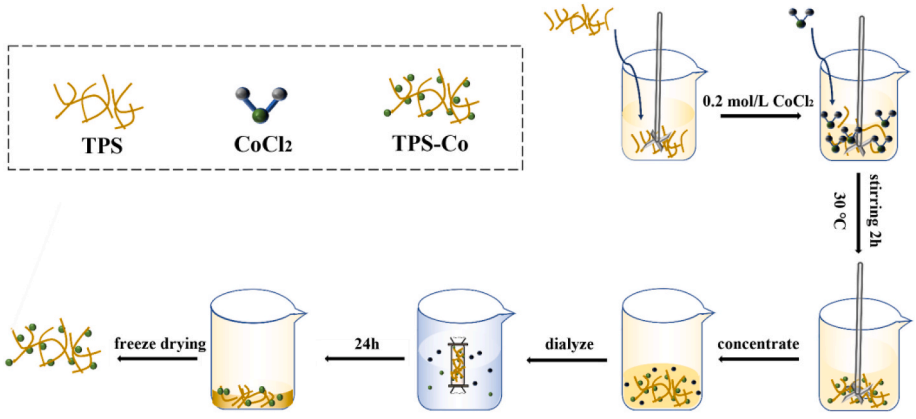

Fig. 1. Schematic illustration for the preparation of TPS-Co.

bathtub. An equal volume of 0.2 mol/L $CoCl_2$ solution was added and reacted in a 30 °C magnetic agitator for 2 h, then concentrated to 20% by volume under reduced pressure using a vacuum rotary evaporator at a temperature of 50 °C. The TPS-Co complex was obtained after 48 h of dialysis and freeze-drying. The specific process is shown in Fig. 1.

2.4. Characterization of TPS and TPS-Co

2.4.1. Molecular weight and determination of cobalt content

The molecular weight and molecular weight distribution of TPS and TPS-Co were determined by high-performance gel filtration chromatography. Their homogeneity was assessed by dissolving 2 mg of TPS and TPS-Co in 400 μL of 0.1 mol/L sodium nitrate solution, respectively. The experimental conditions were a mobile phase of 0.1 mol/L sodium nitrate solution, a flow rate of 0.9 mL/min, and a column temperature of 45 °C. The cobalt content in TPS-Co was detected by Contra700 atomic absorption spectrometer (flame method).

2.4.2. Fourier-transform infrared and ultra-violet spectroscopy analyses

FT-IR measurements were performed with Nicolet 6700 Fourier Transform infrared spectrophotometer in the frequency range of 4000–400 cm^{-1}. The samples were prepared by KBr laminating method, ground with potassium bromide powder and pressed into 1 mm thin slices.

UV absorbance in the 200–400 nm range was measured using an UV–visible spectrophotometer (UV-1800, Shimadzu, Japan).

2.4.3. Thermal performance analysis

Thermogravimetric analysis (TGA) was performed using a synchronous thermal analyzer (STA449F3, NETZSCH, Germany). The samples were recorded at 30–800 °C, protected by 50 mL/min dry nitrogen, and heated at a heating rate of 10/min to analyze the thermal stability of the material.

2.4.4. XRD crystal structure

The crystal structure of TPS and TPS-Co was observed and analyzed using X-ray diffractometry (Empyrean, Netherlands).

2.4.5. X-ray photoelectron spectroscopy

TPS-Co was analyzed by X-ray photoelectron spectrometer (ESCALAB 250Xi thermo Fisher Technology Co., LTD.) to analyze the complexation and elemental valence state.

2.4.6. SEM/EDS

The surface and near surface morphology and structure of TPS and TPS-CO samples were observed and analyzed by field emission scanning electron microscopy (SEM) with X-Max N80 energy spectrometer (JSM-7500F, Japan), and the surface elemental composition of TPS and TPS-Co samples was compared by EDS point scanning.

2.4.7. Atomic force microscopy

Atomic force microscopy (AFM) (Nasoscope, VEECO, USA) was used to precipitate TPS solution (10 μg/mL) and TPS-Co solution (10 μg/mL) on the newly cut surface and detect them under atomic force microscopy.

2.5. Antioxidant activity assays

2.5.1. ABTS radical scavenging activity

According to Kaska et al. [8] and Pereira et al. [9] research method with a slightly modified, ABTS + working solution was obtained by mixing 7.4 mmol/L ABTS solution with 2.6 mmol/L potassium persulfate and reacting in the dark for 12 h. The solution was diluted 40 to 50 times with phosphate buffer pH 7.4 to achieve an absorbance of approximately 0.7 at a wavelength of 734 nm. Then 0.2 mL of different concentrations of samples and 0.8 mL of ABTS + diluted working solution were taken, and after 6 min of reaction at room temperature, the absorbance was measured at 734 nm by enzyme-labeled method. The ABTS + radical scavenging capacity of TPS and TPS-Co was calculated from (Formula 1).

$$\text{ABTS + scavenging ability (\%)} = [1\text{-}(A_1\text{-}A_2)/A_0] * 100 \quad (1)$$

Where A_1 denotes the sample mixed with ABTS + solution, A_2 denotes sample without ABTS + solution, and A_0 is the absorbance of ABTS + solution without the sample as a blank control.

2.5.2. DPPH radical scavenging activity

According to Xiao et al. [10] research method with a slightly modified, weigh 9.85 mg DPPH, dissolve it in anhydrous ethanol, put it in a 250 mL volumetric flask, shake well and prepare a solution with a concentration of 100 μmol/L. Store it at 4 °C for later use. Accurately weigh the sample TPS and TPS-Co 200 mg each, dissolve in 10 mL volumetric flask, add distilled water constant volume, get the standard mother liquor. Take standard mother liquor 0, 0.2, 0.4, 0.6, 0.8 and 1 mL in a 10 mL volumetric bottle. Take the first bottle of solution as blank zero, add 1 mL sample into 3 mL DPPH ethanol solution, mix evenly, and measure the absorbance A_i with

spectrophotometer at 517 nm wavelength after 30 min. At the same time, the absorbance of the mixture of 3 mL DPPH ethanol solution and 1.0 mL sample solvent (A_c) and the absorbance of 3 mL ethanol and 1.0 mL sample (A_b) were measured. The DPPH radical scavenging capacity of TPS and TPS-Co was calculated from (Formula 2) [11].

$$\text{DPPH scavenging ability } (\%) = [1\text{-}(A_i\text{-}A_b)/A_c] *100 \quad (2)$$

Where A_i refers to the sample mixed with DPPH ethanol solution, A_b refers to the sample without DPPH solution, and A_c is the absorbance of DPPH solution without the sample as a blank control.

2.5.3. Hydroxyl radical scavenging activity

According to Chen et al. [12] research method with a slightly modified, For color reaction of ferric sulfate and salicylic acid, 1 mL 9 mmol/L $FeSO_4$ solution was mixed with 1 mL 9 mmol/L salicylic acid ethanol solution, and then 8.8 mmol/L H_2O_2 solution was added. After shaking well, the sample solution was added, and the absorbance was measured at 510 nm. The hydroxyl radical scavenging capacity of TPS and TPS-Co was calculated from (Formula 3).

$$\text{Hydroxyl scavenging ability } (\%) = [1\text{-}(A_i\text{-}A_b)/A_c]*100 \quad (3)$$

Where A_i refers to the sample mixed with working solution, A_b refers to the sample without H_2O_2 solution, and A_c is the absorbance of working solution without the sample as a blank control.

2.6. Proliferation assay of MC3T3-E1 cells

A Cell Counting Kit-8 (CCK-8; Biosharp, China) assay was used to evaluate the cell viability of MC3T3-E1 cells at different concentrations of Co^{2+} in the complete medium (0, 0.5, 1, 2, 3, 4, 10, 20 and 40 ppm), which were prepared with TPS-Co. MC3T3-E1 cells were seeded at a density of 2,000 cells per well (in a 96-well plate) and cultured overnight. The culture medium was next removed and replaced by a medium containing TPS-Co. On day 1, 3, 5 the medium was removed followed by the addition of a 10% CCK-8 solution. After 1-h incubation, the absorbance of each well was measured on a microplate reader at a wavelength of 450 nm. The experiment was repeated 5 times.

3. Statistical analysis

We present all results as the mean ± SD of triplicate. We used Origin 2021 software (Origin Lab Corporation, Northampton, MA, USA) for statistical analysis. One-way ANOVA was performed using SPSS (version 18.0, IBM, Armonk, USA). The difference was defined as statistically significant according to $P < 0.05$.

4. Results

4.1. Characterization of TPS and TPS-Co

4.1.1. Molecular weight and determination of cobalt content

GPC was used to analyze the weight-average (Mw) and number average (Mn) molecular weights, and polydispersity (Mw/Mn) of the TPS and TPS-Co. The results were presented in Table 1. The test results show that the Mw reduced from 110121 g/mol to 73626 g/mol, but the Mw/Mn reduced from 15.66 to 12.11 after complexation. The decrease in Mw indicates that there may be a chain-break effect in TPS-Co, which ultimately led to the formation of heterogeneous molecules. The decrease in Mw/Mn indicates that the molecular weight distribution of TPS-Co was more concentrated than that of TPS. This discrepancy may be due to the incorporation of cobalt in the TPS backbone chain. When a sugar molecule forms a metal complex as a ligand, it is usually one or several monosaccharide units in combination with a metal ion [13,14]. The cobalt content of TPS-Co was measured to be 3.81%, and it showed a part amount of cobalt binds to TPS.

4.1.2. FT-IR and UV spectroscopy analyses

To investigate the binding mode between cobalt and TPS, the FT-IR spectra of TPS and TPS-Co were observed around the 4000-500 cm^{-1} region and presented in Fig. 2A, where the broad stretching peak at 3390 cm^{-1} was ascribed to the hydroxyl groups with stretching vibration. The weak absorption peak at 2935 cm^{-1} was characteristic of C–H stretching vibration. The absorption peak of carbonyl bands at 1743 cm^{-1} indicated the presence of uronic acid in TPS and TPS-Co. The absorption peak at 1622 cm^{-1} was assigned

Table 1
Molecular weight and determination of cobalt content.

	TPS	TPS-Co
Mn	7033	6082
Mw	110121	73626
Mw/Mn	15.66	12.11
Co(%)	–	3.80

to the sugar hydrate [15]. Compared with TPS, the C=O absorption peaks in TPS-Co was red-shifted; this is likely due to the formation of complexes with Co in TPS. The stretching peak at 1021 cm^{-1} indicated the presence of pyranoside, and the absorption peak at 889 cm^{-1} indicated the presence of β-glycosidic bonds in both TPS and TPS-Co [16]. The attenuation of the absorption peak may also be related to the incorporation of cobalt.

The UV spectrum of the TPS and TPS-Co solution in the 200–400 nm range is shown in Fig. 2B. Nucleic acid molecules have a maximum absorption peak at UV 260 nm, indicating the possible presence of nucleic acids in the TPS. However, this peak disappeared with the incorporation of cobalt. This means that the nucleic acids or conjugated protein were removed with the formation of the TPS-Co complex [17].

4.1.3. Thermal property analysis

The TGA distributions of TPS and TPS-Co are shown in Fig. 3A. The weight loss below 220 °C may be due to the physical adsorption of water, and the weight loss between 220 °C and 400 °C may be due to the decomposition of TPS and TPS-Co [18,19]. There is no significant difference between TPS and TPS-Co in terms of physical water absorption. The weight losses for TPS-Co were decreased when compared with that for TPS between 220 °C and 800 °C, which should be ascribed to the complexation between TPS and Co. This shows that TPS-Co has better thermal stability, which is favorable for modification and helps to broaden its application range.

4.1.4. XRD crystal structure

A method to determine the crystal shape and phase composition is via X-ray single-crystal diffraction (XRD). XRD experiments could evaluate the crystallinity of the TPS-Co; Fig. 3B shows the XRD spectrum of TPS and TPS-Co. The high intensity of the XRD peak indicates the relative background intensity and indicates the crystalline phase content. The higher the peak intensity the higher the crystalline phase content [20]. The shift of the XRD peak to the left usually points to a small angular shift, implying a larger lattice constant, probably due to complex Co ions.

4.1.5. X-ray photoelectron spectroscopy

X-ray photoelectron spectroscopy (XPS) measurement was used to provide qualitative information of different surface elements on samples. Fig. 3C, D shows the XPS full scan spectra of TPS and TPS-Co. The Co2p characteristic peak was found in the spectra of TPS-Co, but not in TPS, which can prove that the cobalt was successfully doped into TPS.

4.1.6. SEM/EDS

The typical SEM micrographs of TPS and TPS-Co are presented in Fig. 4(A-D). Fig. 4 shows a significant difference in the microscopic morphology of TPS and TPS-Co, which may be due to the addition of cobalt altering the morphological structure of the TPS. In addition, TPS is fibrous and smoother, while TPS-Co has a slightly rougher structure with depressed structures. These structures increase its surface area and are more conducive to absorption, which may be due to the increase in intermolecular forces after complexation reaction of TPS with cobalt ions, which changes the structural distribution [21]. According to the EDS analysis in Fig. 4E, F, cobalt ions accounted for 3.86% of the total, which is basically the same as previously determined by atomic absorption spectrometry.

4.1.7. AFM imaging analysis

AFM is considered a widely accepted method for direct observation and quantitative characterization of the size and morphology of various types of fixed samples [22]. Fig. 5(A-D) depicts the 2D and 3D AFM images of TPS and TPS-Co. TPS was evenly distributed, but had less aggregation than TPS-Co, with significant variation in particle size. The larger size and more concentrated distribution of TPS-Co indicated that its molecules were more aggregated, which may be related to its stronger intermolecular interactions. This may

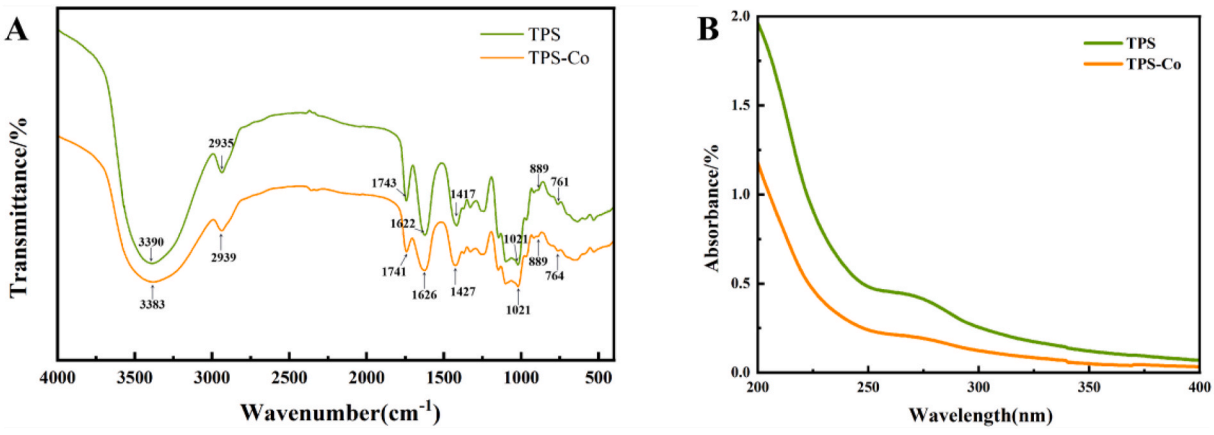

Fig. 2. FT-IR spectra (A) and UV spectra (B) of TPS and TPS-Co.

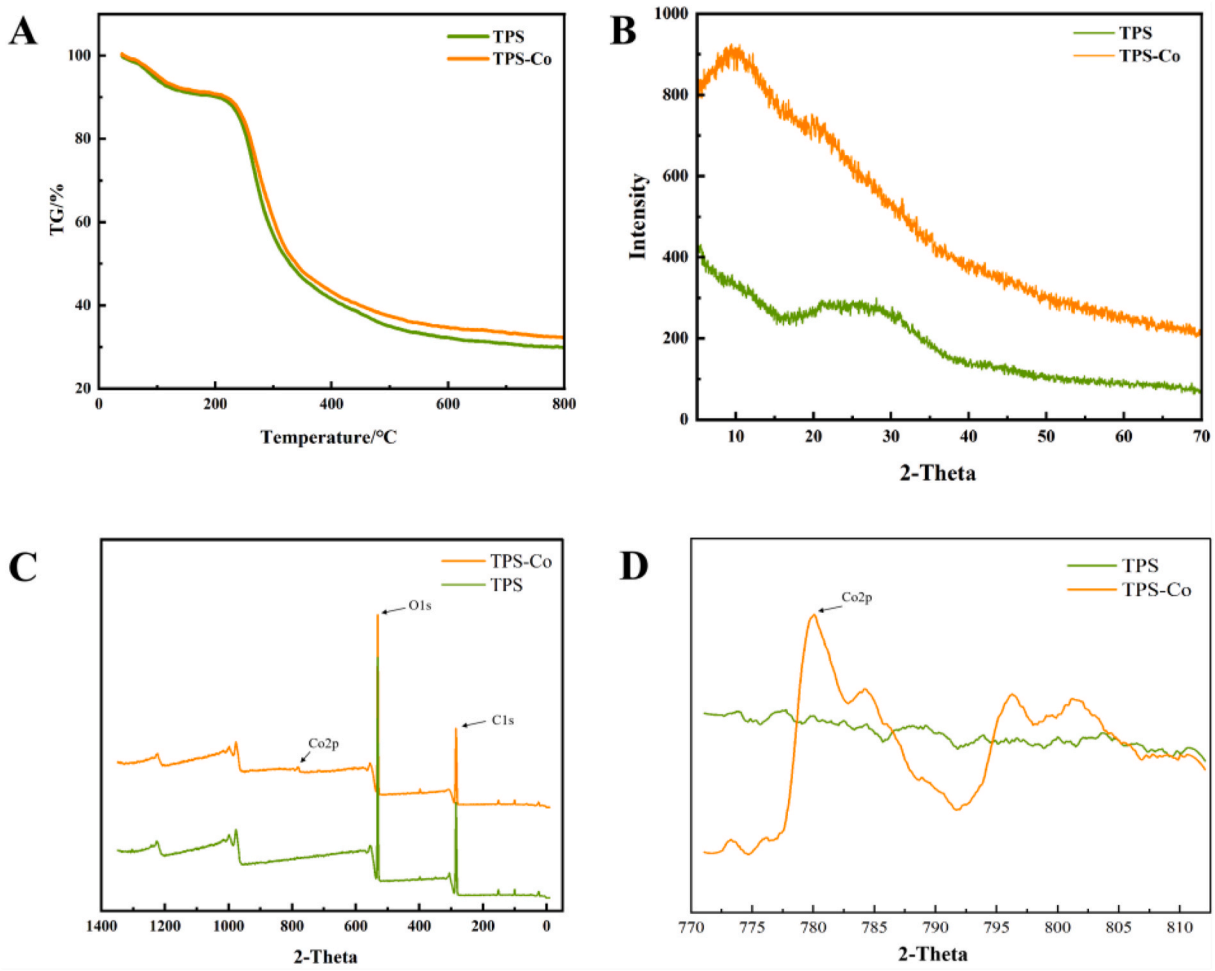

Fig. 3. TGA spectra (30–800 °C) (A), XRD spectra (B), XPS full scan spectra (C) and XPS Co2p spectra (D) of TPS and TPS-Co.

be due to the fact that cobalt changes the spatial structure of the polysaccharide, causing the sugar chains to aggregate together [23]. This is consistent with our results of polydispersity (Mw/Mn) in molecular weight determination.

4.2. Antioxidant activity assays

4.2.1. ABTS radical scavenging activity

The ABTS radical cation (ABTS+) is commonly used to evaluate the total antioxidant activity of single compounds and complex mixtures. Fig. 6A depicts the inhibitory effects of TPS and TPS-Co on ABTS+. At concentrations ranging from 0.4 to 2.0 mg/mL, dose-dependent increases were observed in almost all removal activities. We could observe that the scavenging activity of TPS-Co was higher than that of TPS at all concentrations, suggesting a positive effect of cobaltization on the antioxidant activity. Two factors for this enhanced scavenging activity are: cobalt can interrupt the free radical chain reaction and enhance the antioxidant activity; TPS-Co has a large specific surface area, which can provide many active sites to react with free radicals and inhibit the reaction between free radicals.

4.2.2. DPPH radical scavenging activity

As seen in Fig. 6B, the scavenging ability of both TPS and TPS-Co on DPPH radicals showed a concentration-dependent relationship. The quantitative-effect relationship was obvious when the polysaccharide concentration increased from 0.4 to 2.0 mg/mL. The scavenging rate reached a maximum when the polysaccharide concentration was 2.0 mg/mL. We could observe that the scavenging activity of TPS-Co was higher than that of TPS at all concentrations, suggesting a stronger inhibitory effect of the cobaltized TPS.

4.2.3. Hydroxyl radical scavenging activity

Hydroxyl radicals can cause severe damage to neighboring biomolecules, causing oxidative damage to DNA, lipids and proteins. Therefore, the removal of hydroxyl radicals is essential for the protection of living systems. Polysaccharides enable electron or

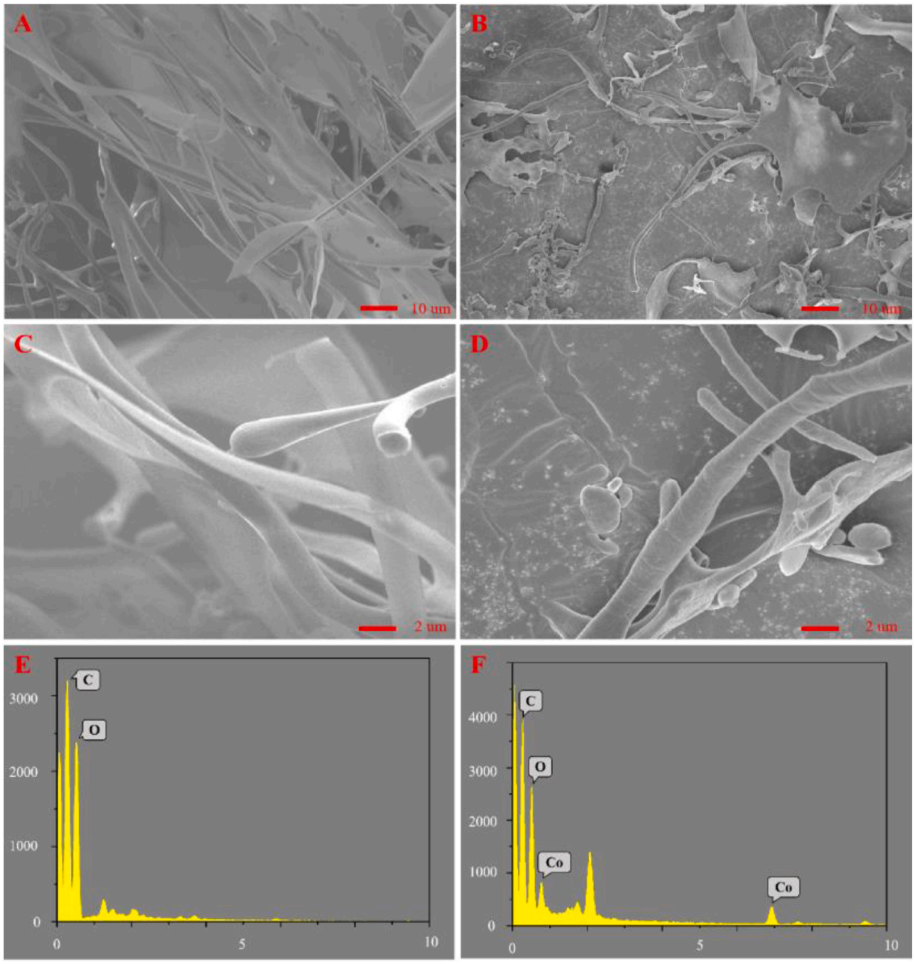

Fig. 4. SEM images for TPS (A, C) and TPS-Co (B, D), EDS for TPS (E) and TPS-Co (F).

hydrogen root donors to scavenge hydroxyl radicals [24]. The scavenging ability of TPS and TPS-Co for hydroxyl radicals is shown in Fig. 6C. Both exhibited hydroxyl radical scavenging activity. A significant quantitative-effect relationship was observed in the concentration range of 0.4–2.0 mg/mL. Similarly, TPS-Co showed better scavenging effect of hydroxyl radicals compared to TPS.

4.3. Effects of TPS-Co on MC3T3-E1 cells proliferation

The cytotoxicity of TPS-Co to MC3T3-E1 cells was evaluated using the CCK-8 assay. The results showed that TPS-Co had no significant cytotoxic effect on MC3T3-E1 at concentrations below 10 ppm (Fig. 6D). It is obvious that TPS-Co could be beneficial to the proliferation of MC3T3-E1 cells. The cell proliferation rate increased with higher concentrations of TPS-Co. However, this proliferation rate decreased as the concentrations of TPS-Co were higher than 2 ppm. The greatest promotion of cell proliferation and viability was observed at a concentration of 2 ppm compared to the control. TPS-Co promoted the viability of MC3T3-E1 cells in a dose-dependent manner. Therefore, we speculated that the optimal concentration to promote MC3T3-E1 cells proliferation is 2 ppm. The optimal concentration of 1 ppm in the previous study by Liu et al. [1] It may be due to the synergistic effect of polysaccharide and cobalt, which reduces the toxic effect of cobalt and up-regulates the safe concentration of cobalt.

5. Discussion

Cobalt is a heavy metal element that is widely distributed around the world. Cobalt is known to be a metal component of vitamin B12 and is essential for the body [25]. Cobalt stimulates the bone marrow hematopoietic system, promotes the production of hemoglobin and increases the number of red blood cells. As a result, $CoCl_2$ has been used to treat anemia and cobalt-based alloys have been used clinically for bone and joint replacement due to their superior mechanical properties. However, numerous studies have shown that excess cobalt ions can cause adverse reactions. High levels of cobalt ions in the body can lead to excessive inflammation and osteolysis [26,27]. Various medical uses of cobalt have been gradually replaced. Therefore, finding a way to mitigate this adverse

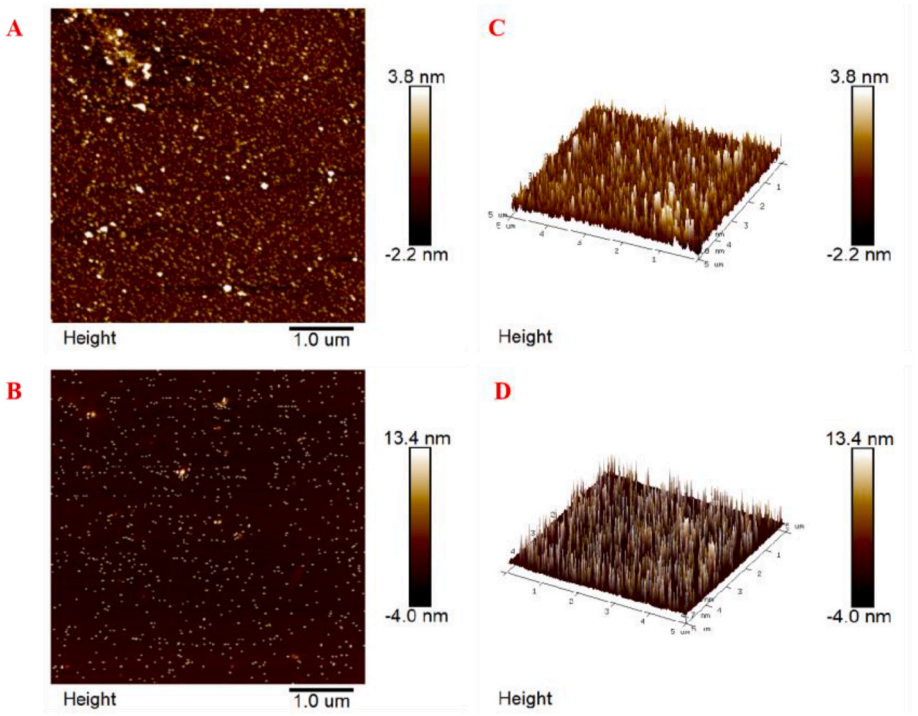

Fig. 5. AFM 2D images of TPS (A) and TPS-Co (B), AFM 3D images of TPS (C) and TPS-Co (D).

reaction while maintaining the excellent physical and chemical properties of cobalt itself would be an effective strategy. In this experiment, TPS was first prepared. In order to synthesize a safer and more effective polysaccode-cobalt complex, cobalt was complexed with the TPS as a complexation platform. To evaluate the physicochemical properties of TPS-Co, we confirmed and characterized the synthesized TPS-Co by various methods.

GPC was used to analyze the weight-average (Mw) and number average (Mn) molecular weights, and polydispersity (Mw/Mn) of the TPS and TPS-Co. This indicates that the molecular weight distribution of TPS-Co is more concentrated than that of TPS, indicating that cobalt complexation has some influence on the structure of TPS. The content of Co in TPS-Co was 3.81% determined by atomic absorption spectrometer, which showed good complexation effect and stability. X-ray photoelectron spectroscopy (XPS) was used to determine the qualitative information of different elements on the surface of TPS-Co. The results show that the characteristic peak of Co2p is found in the spectrum of TPS-Co, but not in TPS, which can prove the successful doping of cobalt into TPS. Infrared spectroscopy results showed the influence of cobalt on the structure of TPS. Compared with TPS, the C═O absorption peak in TPS-Co was redshifted. This may be due to the formation of carbonyl complexes with Co in TPS. Ultraviolet spectra indicated that the nucleic acid or conjugate protein of TPS-Co complex was largely removed after adding cobalt. The TGA results showed that the thermal stability was improved after complexation of TPS with Co, making further improvement of TPS-Co functionalization possible. The crystal structure of TPS-Co was determined by XRD. Typical SEM micrographs of TPS and TPS-Co show that TPS is fibrous and smooth, whereas TPS-Co has a slightly rough depressed structure. These structures increase its surface area and may allow it to have better biological effects. AFM images suggest that the addition of cobalt may alter the spatial structure of the TPS. Antioxidant experiments showed that TPS-Co was superior to TPS in scavenging ABTS, DPPH and Hydroxyl radicals. Finally, we analyzed the effect of prepared TPS-Co on the proliferation of MC3T3-E1 cells. Based on the results of CCK-8 assay, we speculated that the optimal cobalt concentration for TPS-Co to promote the proliferation of MC3T3-E1 cells was 2 ppm. The optimal cobalt concentration for $CoCl_2$ in a previous study by Liu et al. was 1 ppm [1]. This may be due to the synergistic effect of polysaccharides and cobalt, which reduces the toxic effect of cobalt, improves the safe concentration of cobalt, and still ensures its ability to promote bone regeneration, proving that our strategy is successful. In conclusion, compared with TPS, TPS-Co may have better physical and chemical properties, and the conversion of inorganic cobalt into organic cobalt may be an effective strategy. We prove that there may be more strategies to solve the paradoxical effects like cobalt, so that their excellent properties are not buried. In the future, more attempts should be made to explore the application of Co and more potential value.

6. Conclusions

In this study, we complexed Co with TPS to prepare a new metal-polysaccharide complex, TPS-Co. Structural characterization results showed that cobalt complexes successfully with TPS, while TPS-Co is more homogeneous and concentrated with higher thermal stability compared to TPS. Antioxidant activity assays showed that TPS-Co has better antioxidant activity than TPS in the

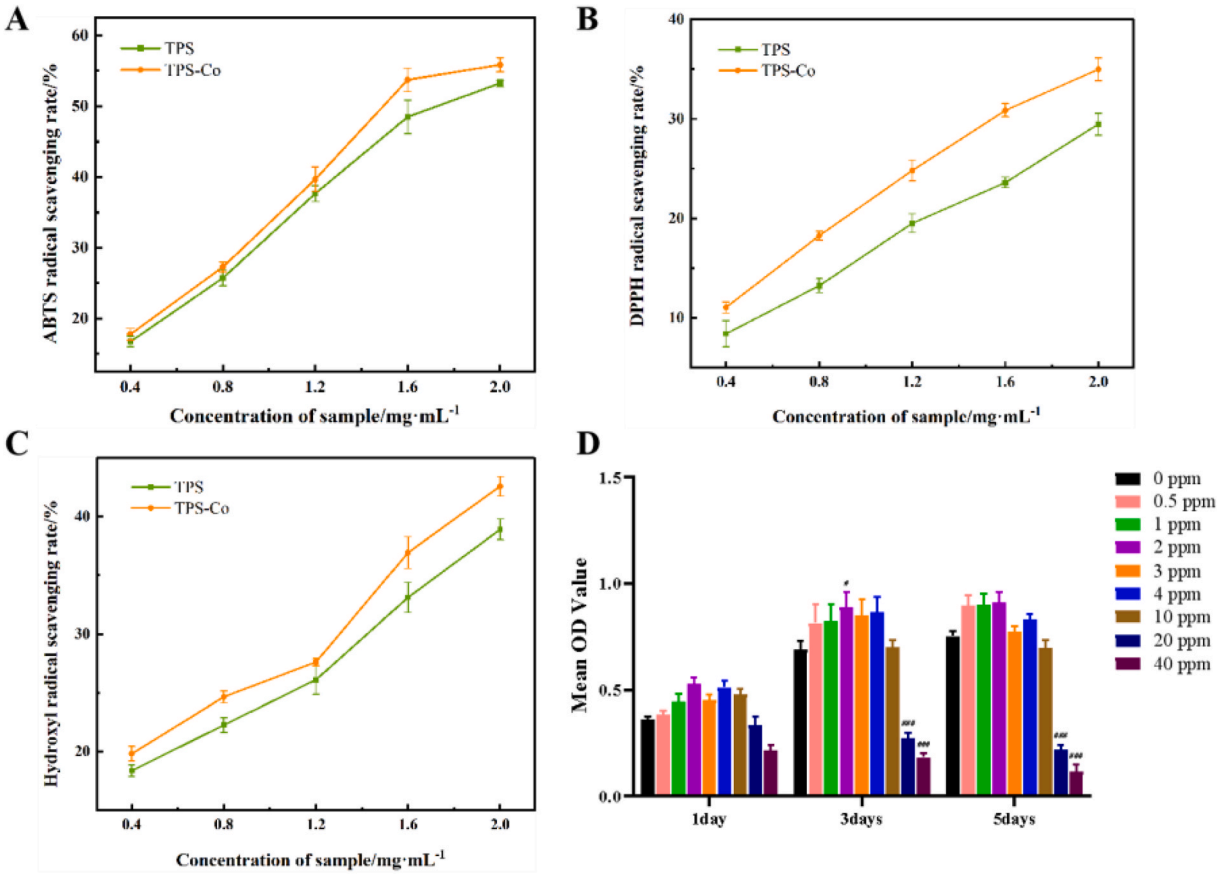

Fig. 6. (A) ABTS radical scavenging, (B) DPPH radical scavenging and (C) Hydroxyl radical scavenging of TPS and TPS-Co, (D) The CCK-8 assay detects proliferation of MC3T3-E1 cells. The values shown are the mean SEM of five replicates. (*$p < 0.05$ or ***$p < 0.001$ stands for a significant difference compared with 0 ppm groups.)

concentration range of 0.4–2 mg/mL. Proliferation assay of MC3T3-E1 cells demonstrated that TPS-Co has the best cell proliferation effect at a cobalt concentration of 2 ppm. It showed that the combination of TPS with Co can effectively increase the safe concentration of cobalt. TPS-Co may have potential applications in bone regeneration.

Author contribution statement

Hongfu Zhou: Conceived and designed the experiments; Performed the experiments.
Yong Chen: Conceived and designed the experiments; Performed the experiments; Wrote the paper.
Ziyao Wang, Chen Xie, Dan Ye, Anran Guo, Wenjing Xie, Jun Xing: Analyzed and interpreted the data.
Min Zheng: Conceived and designed the experiments; Contributed reagents, materials, analysis tools or data.

Data availability statement

The authors do not have permission to share data.

Declaration of interests statement

The authors declare no conflict of interest.

Acknowledgements and Funding Statement

We would like to thank Dr. Tao Chen and Dr. Juntao Wang for their assistance in the experiment and imaging, and also thank the Key Project of Scientific Instruments of the National Natural Science Foundation of China (Project No. 81727805), the Scientific Research Program of the Department of Education of Hubei Province (B2019159), the Doctoral Initiation Fund Project (BK201803,

BK202307), and the Scientific Research Program of the Department of Education of Hubei Province. Supported by the project of Hundred Schools and Hundred Counties (BXLBX0794, BXLBX0795), the Key Project of Science and Technology Research and Development of Xianning City (2021SFYF003), Innovation team of Hubei University of Science and Technology (2023T10).

References

[1] G. Liu, X. Wang, X. Zhou, L. Zhang, J. Mi, Z. Shan, B. Huang, Z. Chen, Z. Chen, Modulating the cobalt dose range to manipulate multisystem cooperation in bone environment: a strategy to resolve the controversies about cobalt use for orthopedic applications, Theranostics 10 (3) (2020) 1074–1089, https://doi.org/10.7150/thno.37931.
[2] Q. Ding, W. Zheng, B. Zhang, X. Chen, J. Zhang, X. Pang, Y. Zhang, D. Jia, S. Pei, Y. Dong, B. Ma, Comparison of hypoglycemic effects of ripened pu-erh tea and raw pu-erh tea in streptozotocin-induced diabetic rats, RSC Adv. 9 (6) (2019) 2967–2977, https://doi.org/10.1039/c8ra09259a.
[3] X. Miao, H. Ma, Q. Ke, S. Wang, H. Zhou, M. Zheng, The determination of monosaccharide in different years Qingzhuan Dark Tea polysaccharide by liquid chromatography-mass spectrometry, Phytochem. Anal. 33 (4) (2022) 577–589, https://doi.org/10.1002/pca.3111.
[4] Z. Qi, Z. Le, F. Han, Y. Feng, M. Yang, C. Ji, L. Zhao, Inhibitory regulation of purple sweet potato polysaccharide on the hepatotoxicity of tri-(2,3-dibromopropyl) isocyanate, Int. J. Biol. Macromol. 194 (2021) 445–451, https://doi.org/10.1016/j.ijbiomac.2021.11.086.
[5] Y. Peng, F. Ma, L. Hu, Y. Deng, W. He, B. Tang, Strontium based Astragalus polysaccharides promote osteoblasts differentiation and mineralization, Int. J. Biol. Macromol. 205 (2022) 761–771, https://doi.org/10.1016/j.ijbiomac.2022.03.088.
[6] N. Yehuda, Y. Turkulets, I. Shalish, A. Kushmaro, S. (Malis) Arad, Red microalgal sulfated polysaccharide-Cu_2O complexes: characterization and bioactivity, Acs. Appl. Mater. Inter. 13 (6) (2021) 7070–7079, https://doi.org/10.1021/acsami.0c17919.
[7] H. Zhou, Z. Wang, Q. Ke, S. Wang, Y. Chen, C. Xie, C. Wang, M. Zheng, Preparation and characterisation of Qingzhuan dark tea polysaccharide–zinc, Food Sci. Tech-Brazil. 42 (2022), e32022, https://doi.org/10.1590/fst.32022.
[8] A. Kaska, N. Deniz, M. Çiçek, R. Mammadov, The screening of Digitalis ferruginea L. subsp. ferruginea for toxic capacities, phenolic constituents, antioxidant properties, mineral elements and proximate analysis, Food Sci. Tech-Brazil. 41 (2) (2020) 505–512, https://doi.org/10.1590/fst.08620.
[9] I. Pereira, J. Matos Neto, R. Figueiredo, J. Carvalho, E. Figueiredoet, N. Menezes, S. Gabanal, Physicochemical characterization, antioxidant activity, and sensory analysis of beers brewed with cashew peduncle (Anacardium occidentale) and orange peel (Citrus sinensis), Food Sci. Tech-Brazil. 40 (3) (2020) 749–755, https://doi.org/10.1590/fst.17319.
[10] H. Xiao, X. Fu, C. Cao, C. Li, C. Chen, Q. Huang, Sulfated modification, characterization, antioxidant and hypoglycemic activities of polysaccharides from Sargassum pallidum, Int. J. Biol. Macromol. 121 (2018) 407–414, https://doi.org/10.1016/j.ijbiomac.2018.09.197.
[11] H. Zhou, C. Xie, Z. Wang, Y. Chen, D. Ye, A. Guo, W. Xie, J. Xing, C. Wang, M. Zheng, Preparation, characterization and antioxidant activity of polysaccharides copper from Qingzhuan dark tea, Food Sci. Tech-Brazil 43 (2023), https://doi.org/10.1590/fst.102322.
[12] S. Ben Slima, N. Ktari, I. Trabelsi, H. Moussa, I. Makni, R. Ben Salah, Purification, characterization and antioxidant properties of a novel polysaccharide extracted from Sorghum bicolor (L.) seeds in sausage, Int. J. Biol. Macromol. 106 (2017) 168–178, https://doi.org/10.1016/j.ijbiomac.2017.08.010.
[13] J. Rendleman, Metal-polysaccharide complexes—Part I, Food Chem. 3 (1) (1978) 47–79, https://doi.org/10.1016/0308-8146(78)90047-X.
[14] J. Rendleman, Metal-polysaccharide complexes—Part II, Food Chem. 3 (2) (1978) 127–162, https://doi.org/10.1016/0308-8146(78)90031-6.
[15] Y. Gu, Y. Qiu, X. Wei, Z. Li, Z. Hu, Y. Gu, Y. Zhao, Y. Wang, T. Yue, Y. Yuan, Characterization of selenium-containing polysaccharides isolated from selenium-enriched tea and its bioactivities, Food Chem. 316 (2020), 126371, https://doi.org/10.1016/j.foodchem.2020.126371.
[16] M. Meng, D. Cheng, L. Han, Y. Chen, C. Wang, Isolation, purification, structural analysis and immunostimulatory activity of water-soluble polysaccharides from Grifola Frondosa fruiting body, Carbohydr. Polym. 157 (2016) 1134–1143, https://doi.org/10.1016/j.carbpol.2016.10.082.
[17] Y. Peng, F. Ma, L. Hu, Y. Deng, W. He, B. Tang, Strontium based Astragalus polysaccharides promote osteoblasts differentiation and mineralization, Int. J. Biol. Macromol. 205 (2022) 761–771, https://doi.org/10.1016/j.ijbiomac.2022.03.088.
[18] G. Leone, M. Consumi, S. Lamponi, C. Bonechi, G. Tamasi, A. Donati, C. Rossi, A. Magnani, Thixotropic PVA hydrogel enclosing a hydrophilic PVP core as nucleus pulposus substitute, Mat. Sci. Eng. C-Mater. 98 (2019) 696–704, https://doi.org/10.1016/j.msec.2019.01.039.
[19] G. Leone, A. Bidini, S. Lamponi, A. Magnani, States of water, surface and rheological characterisation of a new biohydrogel as articular cartilage substitute, Polym. Adv. Technol. 24 (9) (2013) 824–833, https://doi.org/10.1002/pat.3150.
[20] N. Kadum, Z. Al-Azzawi, T. al-Attar, T. Al-Attar, M. Al-Neami, W. AbdulSahib, XRD analysis for hydration products of different lime-pozzolan systems, MATEC Web Conf. 162 (2018), 02007, https://doi.org/10.1051/matecconf/201816202007.
[21] J. Dong, H. Li, W. Min, Preparation, characterization and bioactivities of Athelia rolfsii exopolysaccharide-zinc complex (AEPS-zinc), Int. J. Biol. Macromol. 113 (2018) 20–28, https://doi.org/10.1016/j.ijbiomac.2018.01.223.
[22] Y. Zhu, Y. Chen, Q. Li, T. Zhao, M. Zhang, W. Feng, M. Takase, X. Wu, Z. Zhou, L. Yang, X. Wu, Preparation, characterization, and anti-Helicobacter pylori activity of Bi3+-Hericium erinaceus polysaccharide complex, Carbohydr. Polym. 110 (2014) 231–237, https://doi.org/10.1016/j.carbpol.2014.03.081.
[23] L. Wang, H. Liu, G. Qin, Structure characterization and antioxidant activity of polysaccharides from Chinese quince seed meal, Food Chem. 234 (2017) 314–322, https://doi.org/10.1016/j.foodchem.2017.05.002.
[24] S. Khaskheli, W. Zheng, S. Sheikh, A. Khaskheli, Y. Liu, A. Soomro, X. Feng, M. Sauer, Y. Wang, W. Huang, Characterization of Auricularia auricula polysaccharides and its antioxidant properties in fresh and pickled product, Int. J. Biol. Macromol. 81 (2015) 387–395, https://doi.org/10.1016/j.ijbiomac.2015.08.020.
[25] R. Edward, Vitamin B12, folic acid, and the nervous system, Lancet Neurol. 5 (2006) 949–960, https://doi.org/10.1016/S1474-4422(06)70598-1.
[26] G. Bradford D, S. Thomas, W. Erik, T. Stephen S, A systematic review of systemic cobaltism after wear or corrosion of chrome-cobalt hip implants, J. Patient Saf. 15 (2019) 97–104, https://doi.org/10.1097/PTS.0000000000000220.
[27] L. Laura, V. Bart, V.D.S. Catherine, W. Floris, M. Leen, Cobalt toxicity in humans-A review of the potential sources and systemic health effects, Toxicology 387 (2017) 43–56, https://doi.org/10.1016/j.tox.2017.05.015.